Electronic Supplementary Information: *Ab initio* Investigation of the Role of Transition-metal Dopants in the Adsorption Properties of Ethylene Glycol on Doped Pt(100) Surfaces

Raquel C. Bezerra,[*,†] Paulo C. D. Mendes,[*,‡] Raimundo R. Passos,[*,†] and Juarez L. F. Da Silva[*,‡]

†*Departament of Chemistry, Federal University of Amazonas, Av. General Rodrigo Octávio,* 6200*, Coroado I,* 69080-900*, Manaus, AM, Brazil*

‡*São Carlos Institute of Chemistry, University of São Paulo, PO Box* 780*,* 13560-970*, São Carlos, SP, Brazil*

E-mail: racosbez@gmail.com; paulaocdm@gmail.com; rrpassos@ufam.edu.br; juarez_dasilva@iqsc.usp.br

1 Introduction

The present electronic supplementary material contains several additional information, which are listed below:

- Additional technical details on VASP calculations.

- Results (relative energies, electronic states, effective Bader charges) for all calculated ethylene glycol isomers.
- Computational convergence calculations for clean and doped surfaces.
- Results for all calculated configurations for the adsorbed systems, i.e., Tables and Figures.

2 Computational Details: PAW-PBE Projectors

In Table S1, we provide information about the Projector Augmented Wave (PAW) projectors employed in the study.

Table S1: Most important parameters for the selected PAW-PBE projectors: chemical species, selected PAW projector, number of valence electrons, Z_{val}, and the recommended plane-wave cutoff energy indicated by `ENMAX` in the respective `POTCAR` file.

Element	PAW-PBE `POTCAR`	Z_{val}	`ENMAX` (eV)
H	H_GW 21Apr2008	1	300.000
C	C_GW_new 19Mar2012	4	413.992
O	O_GW 19Mar2012	6	434.431
Fe	Fe_GW 31Mar2010	8	321.007
Co	Co_GW 31Mar2010	9	323.400
Ni	Ni_GW 31Mar2010	10	357.323
Ru	Ru_sv_GW 05Dec2013	16	348.106
Rh	Rh_GW 06Mar2008	9	247.408
Pd	Pd_GW 06Mar2008	10	250.925
Pt	Pt_GW 10Mar2009	10	248.408

3 Convergence Tests: Bulk Pt in the Face-centered Cubic Structure

In Figure S1, we show the variation in the lattice parameter, Δa_0 in %, and relative energy, ΔE_{tot} in meV, with respect to the highest value employed for the plane-wave cutoff energy

and number of **k**-points (represented here by the **k**-mesh), while the local density of states for bulk Pt is shown in Figure S2.

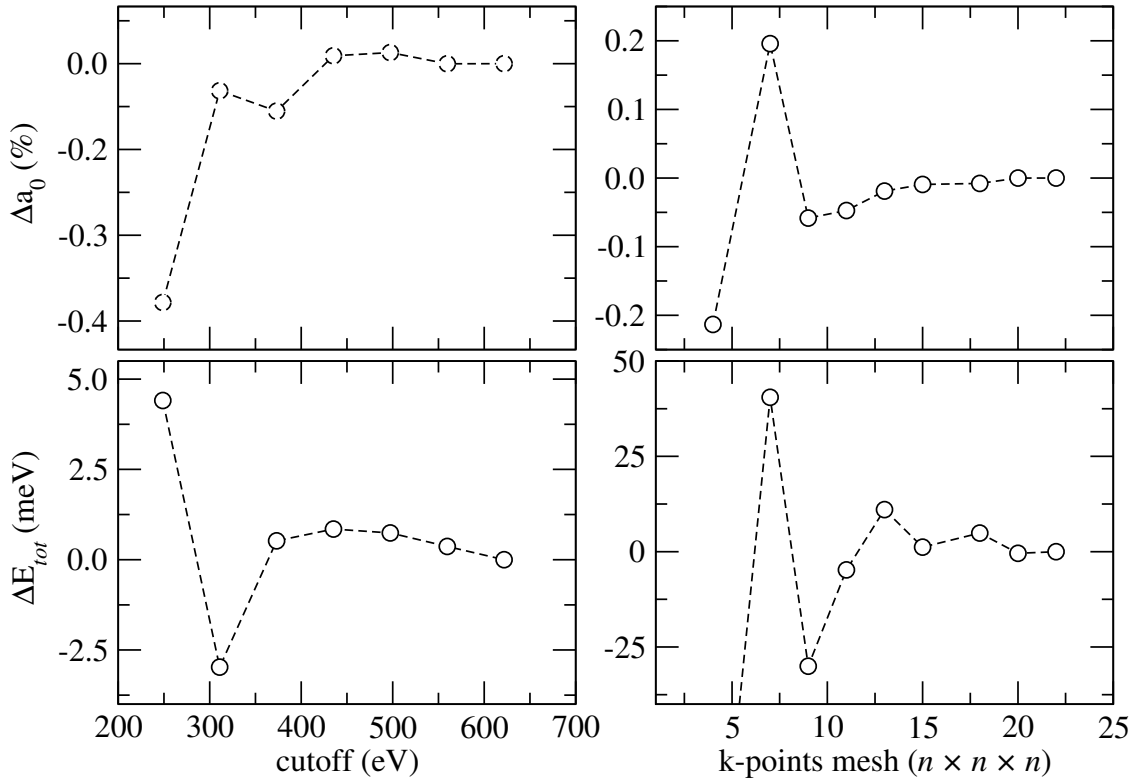

Figure S1: Convergence tests for the lattice parameter and total energy with respect to the plane-wave cutoff energy and k-mesh for face-centered cubic Pt bulk.

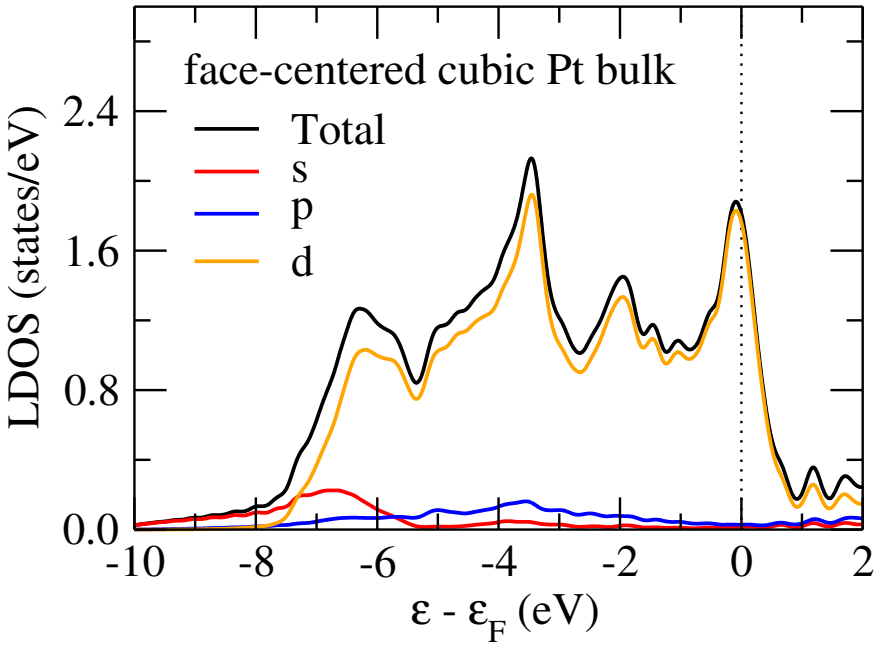

Figure S2: Local density of states (LDOS) for bulk Pt in the face-centered cubic structure. The total density of states (black line) is decomposed into s- (red line), p- (blue line) and d-states (orange line). The Fermi energy is indicated by the vertical dashed line.

4 Gas-phase Ethylene Glycol

Several isomers of the ethylene glycol, which are reported in the literature as geometrically unique are showed in Figure S3. For the main text, we employed clustering techniques (k-means), which allow us to group the configurations considering different properties, such as energetic and structural. Then, based on the total energy and atomic coordinates of the EG isomers, we separated the configurations into four group and we presented, in Figure 1 of the manuscript, the lowest energy configuration of each group. Figure S4 shows two selected EG isomers and the effective Bader charges on each atom. Figure S5 shows the density of states of gas-phase ethylene glycol for the two isomers that were employed in the adsorption studies. Finally, we provide a list of atomic cartesian coordinates for the EG isomers, which can be distinguished by the relative total energies.

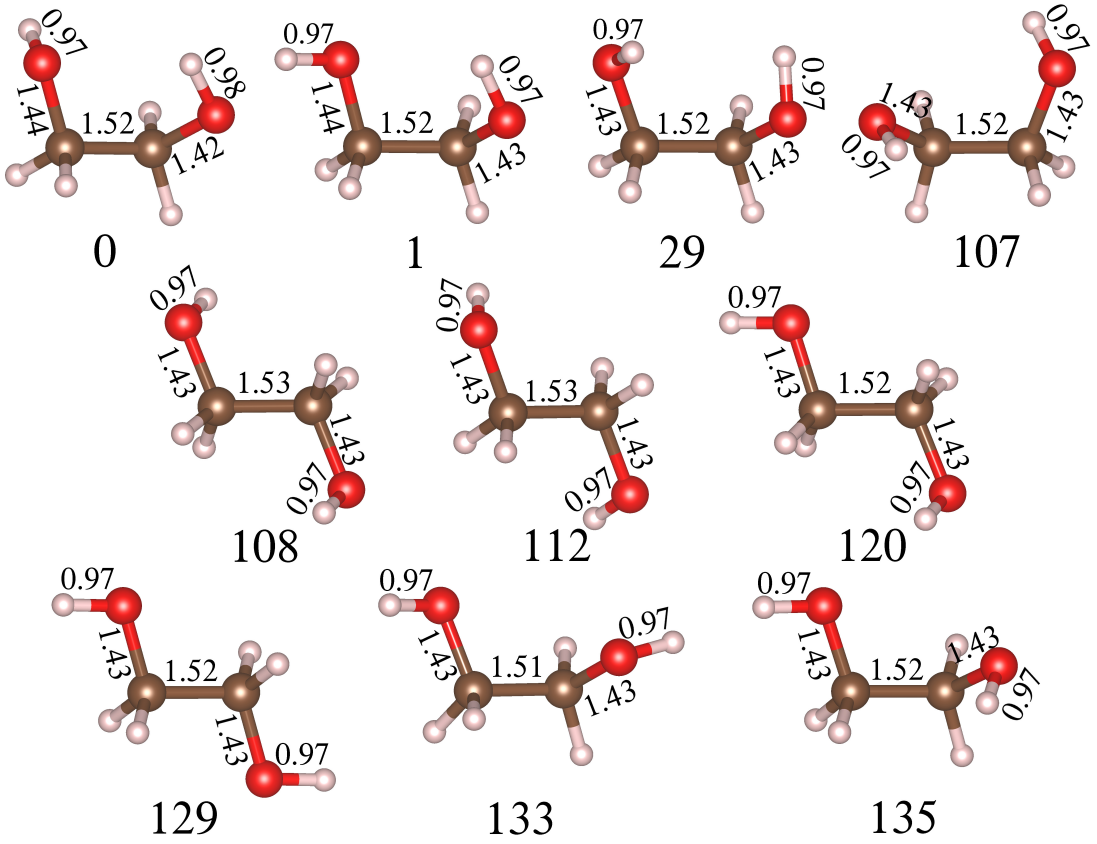

Figure S3: Conformational isomers of the ethylene glycol in the gas phase with the C−C, C−O and O−H bond lengths in Å and the relative energies with respect to the lowest energy configuration in meV.

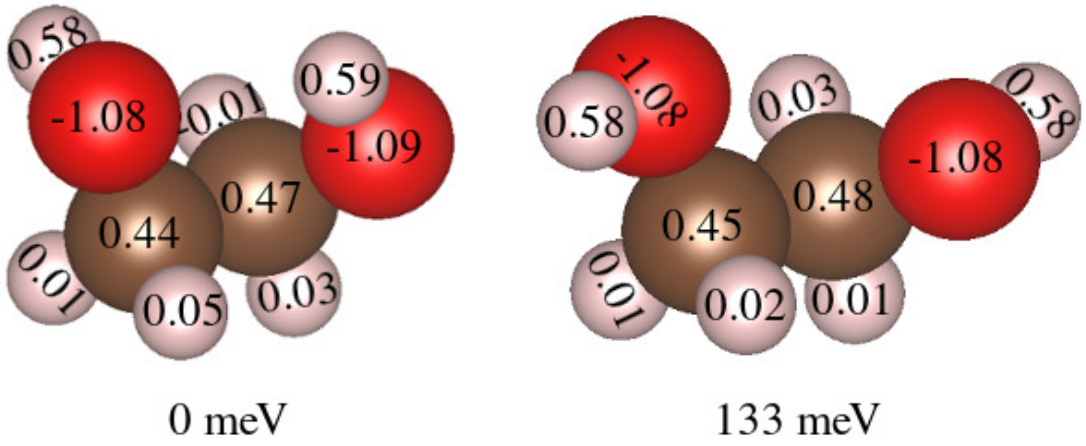

Figure S4: Structures for selected ethylene glycol isomers showing the effective Bader charges for each atom. Below the structures are the relative energies with respect to the lowest energy ethylene glycol configuration in our set.

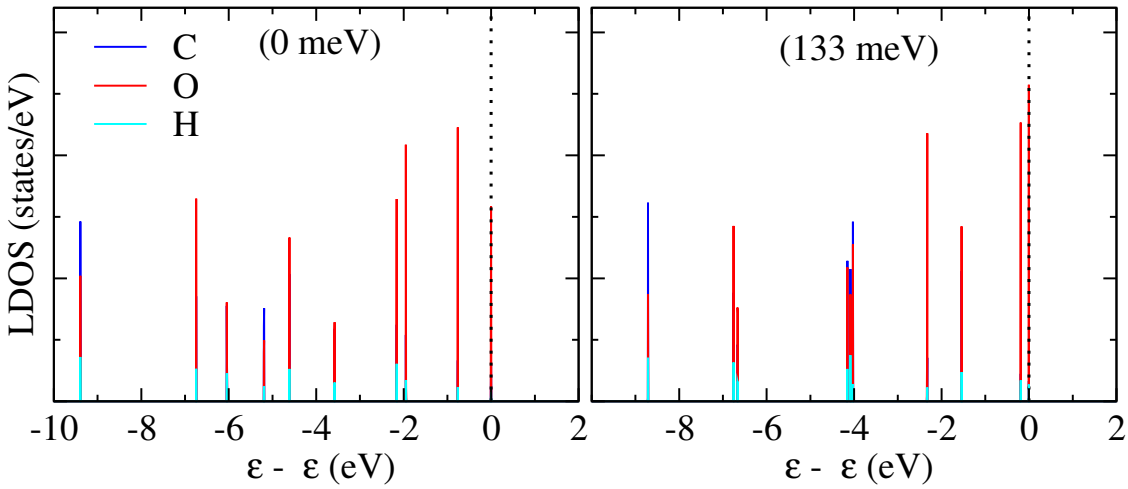

Figure S5: local density of states (LDOS) of the two isolated isomers of ethylene glycol, distinguished by the energy relative to the lowest energy structure (indicated between parentheses), employed to study the different adsorption modes discussed in the main article.

Below we provide the cartesian atomic coordinates of the isomers calculated, indicating the total energy, in eV, and the relative total energy (with respect to the lowest energy configuration), in meV.

$E_{tot} = -53.333\,754\,00\,\text{eV},\ \Delta E_{tot} = 135\,\text{meV}$

C -0.1776123242835332 0.2129167627359392 -0.8670294959265674

C -0.1815824723628063 0.2063511482357168 0.6509923925464238

O 1.1637532547594835 0.2485333628931725 1.1261323811580275

O 0.3878381680318315 -0.9544465984517929 -1.4603739227739871

H 1.1469356360490206 0.1960104424138693 2.0949137983623483

H -0.0922861092354950 -1.7275326196634149 -1.1186860978601749

H -0.7606851195955251 1.0852202256778760 0.9983213901849246

H -0.7067684143025916 -0.7018379297437143 1.0139113614737210

H -1.2161622548544022 0.3813125671626523 -1.2150505942762719

H 0.4365696357940179 1.0534726387396960 -1.2231312128884437

$E_{tot} = -53.336\,536\,96\,\text{eV},\ \Delta E_{tot} = 133\,\text{meV}$

C -0.2284709433065206 0.1674950505739075 -0.7562495613261669

C -0.2283712569874901 0.1676044673462966 0.7562704529469674

O 1.1238203843145929 0.2020376330863165 1.2231344035483802

O 0.1449055284979490 -1.1325554831475211 -1.2231341194496639

H 1.1267316890589036 -0.0342319631344230 2.1640050095180992

H 0.3709195265288807 -1.0644134262735090 -2.1640623744817962

H -0.7918064262750573 1.0538172612495460 1.1081495732475541

H -0.7532462064890515 -0.7390049496120872 1.1095630512740493

H 0.4785278160369728 0.9405535367656297 -1.1095510822751788

H -1.2430101113791796 0.4386978731458440 -1.1081253530022441

$E_{tot} = -53.340\,060\,29\,\text{eV},\ \Delta E_{tot} = 129\,\text{meV}$

C 0.0043950603577221 0.0000000000000007 -0.7594276094538954

C -0.0043950603578073 0.0000000000000007 0.7594276094538954

O 1.3621435529098553 0.0000000000000007 1.1859960059889763

O -1.3621435529098029 0.0000000000000007 -1.1859960059889763

H 1.3751051279645949 0.0000000000000007 2.1559608428579735

H -1.3751051279646758 0.0000000000000007 -2.1559608428579735

H -0.5453527220802261 -0.8945372829348690 1.1187090936103572

H -0.5453527220802261 0.8945372829348670 1.1187090936103572

H 0.5453527220802830 -0.8945372829348690 -1.1187090936103572

H 0.5453527220802830 0.8945372829348670 -1.1187090936103572

$E_{tot} = -53.349\,383\,00\,\mathrm{eV},\ \Delta E_{tot} = 120\,\mathrm{meV}$

C 0.0373932271354973 0.0723383523391908 -0.8588916262478921

C 0.0309875814814267 0.0727219418160975 0.6652936347542258

O 1.3940476518309777 0.0676233382838588 1.1009257247353230

O -1.2870043581372868 0.0900806617796402 -1.3953571164361924

H 1.4033004254818473 0.1251824359737642 2.0694344731101775

H -1.7089602139590119 -0.7599336421846979 -1.1866715828475551

H -0.5124969122482235 0.9648209523994823 1.0256809432656442

H -0.5080096958344857 -0.8249468337552400 1.0309600715734155

H 0.5299314415107728 0.9840745722780831 -1.2262775851408860

H 0.6208108527384861 -0.7919617789301791 -1.2250969367662603

$E_{tot} = -53.356\,833\,32\,\mathrm{eV},\ \Delta E_{tot} = 112\,\mathrm{meV}$

C 0.0094292764715447 -0.1410459675124698 -0.7642151018859531

C 0.0017131409176634 -0.1413333401404837 0.7642239755631888

O 1.3195696475865941 -0.1288034367093505 1.3150269334580491

O -1.3053076121882607 -0.2324415870686170 -1.3150366543573364

H 1.7550863063611248 0.6959936654882282 1.0413400346427029

H -1.8044835236794172 0.5554668999148116 -1.0413672585133247

H -0.4752866118592054 -1.0611091123340421 1.1317257230702928

H -0.5993232099082986 0.7143324755849023 1.1350306861056305

H 0.5411752225753035 0.7593175812643715 -1.1350304423246635

H 0.5574273637229514 -1.0203771784873505 -1.1316978957585864

$E_{tot} = -53.360\,931\,52\,\mathrm{eV}$, $\Delta E_{tot} = 108\,\mathrm{meV}$

C -0.0013656515880559 -0.0022922013242989 -0.7647371657588428

C 0.0013656515879697 0.0022922013242465 0.7647371697589337

O 1.3263774939322244 0.0048466410435332 1.3029138761047192

O -1.3263774939321642 -0.0048466410435900 -1.3029138821047976

H 1.7283590525525212 0.8677043125748295 1.1079639730430384

H -1.7283590525524655 -0.8677043125747576 -1.1079639690429339

H -0.5983717303605932 0.8550216579272384 1.1322185468676875

H -0.4706531580208809 -0.9193793707898058 1.1419609312212713

H 0.4706531580207948 0.9193793707898955 -1.1419609272213045

H 0.5983717303606492 -0.8550216579272908 -1.1322185528677704

$E_{tot} = -53.361\,782\,20\,\mathrm{eV}$, $107\,\mathrm{meV}$

C -0.2850279771493059 -0.1232520176329789 -0.7608113507035194

C -0.2864330872854027 -0.1198344966964860 0.7614176706680013

O 1.0071059064976415 -0.2110800912076417 1.3537709453059681

O 0.5476741505582671 0.8705374422390121 -1.3531400604525452

H 1.5138179131480598 -0.8850820562414720 0.8696446222460267

H 0.4108463870591860 1.7047258786192332 -0.8725585256726361

H -0.9525188623456372 -0.9372409951734019 1.1059378292823490

H -0.7162052063020320 0.8250235249476477 1.1369688396748505

H 0.0964623436428901 -1.0886854821153957 -1.1360360684117394

H -1.3357215678236667 -0.0351117067385166 -1.1051939019367547

$E_{tot} = -53.439\,896\,71\,\text{eV},\ \Delta E_{tot} = 29\,\text{meV}$

C -0.3662942669935609 0.2073007927709702 -0.7609137105626811

C -0.3776198684321108 0.1859228571930660 0.7610337325764789

O 0.9465763991974563 0.2343032501618292 1.3073249130420113

O 0.3392145164237825 -0.9142449049611012 -1.3071390150341138

H 1.3189325075100622 -0.6596947939823461 1.2310173993501978

H 1.2878326443547050 -0.7181329174651174 -1.2316499984171907

H -0.9052896732875948 1.0755753650816025 1.1393898838637524

H -0.9159748450035665 -0.7104698015043120 1.1184176425005194

H 0.0712816987566023 1.1569307712860266 -1.1182340929729966

H -1.3986591125257752 0.1425093814193823 -1.1392467543459777

$E_{tot} = -53.468\,251\,33\,\text{eV},\ \Delta E_{tot} = 1\,\text{meV}$

C -0.3333196822762998 0.1650840302971064 -0.8749373726888723

C -0.3401315210876890 0.1676450173446504 0.6415762865892414

O 1.0353208221617436 0.2011244143240871 1.0609746687179631

O 0.3239252653600175 -0.9839865789615958 -1.4032319580424448

H 1.0819923478048974 -0.0674405225980150 1.9916933801847168

H 1.1872225436690940 -1.0273262844509672 -0.9537373297774701

H -0.8908976235953494 1.0516746790909677 1.0153741880120246

H -0.8394723588961241 -0.7461674236294851 1.0098362811998771

H -1.3676256001992595 0.1427889833532676 -1.2490710042133570

H 0.1429858070589693 1.0966036852299839 -1.2384771399816787

$E_{tot} = -53.469\,141\,61\,\text{eV}$, $\Delta E_{tot} = 0\,\text{meV}$

C -0.3686227863524483 0.0497585864554089 -0.7971958076053300

C -0.3691754587496021 0.0554229967943880 0.7235958483665059

O 0.9728625274492853 0.0794831783463494 1.2391367872669155

O 0.3753203513493286 -1.0454624623108384 -1.3203600934994877

H 1.3408399616621836 0.9644009380486378 1.0732352021016642

H 1.1876192013169984 -1.0969649150935352 -0.7826385512911540

H -0.9663041753534563 0.9030352410265423 1.1072882197630460

H -0.8084182105319293 -0.8787462497300098 1.1030881616390595

H -1.3984875934310637 -0.0466788066606612 -1.1758941104183331

H 0.0343661826407038 1.0157514931237182 -1.1702556563228863

5 Convergence of the Clean Surface Properties for the Undoped Pt(100) Substrate versus the Number of Layers in the Slab

The surface energy, σ, was obtained using Equation S1:

$$\sigma = \frac{1}{2}(E_{tot}^{\text{slab}} - N \times E_{tot}^{\text{bulk}}) \ , \tag{S1}$$

where E_{tot}^{slab} is the total energy of the slab (1×1 unit cell), N is the number of layers and E_{tot}^{bulk} is the total energy per atom for the bulk. The term E_{tot}^{bulk} was obtained through two distinct methods: (*i*) from a separate DFT calculation using a bulk unit cell (indicated by circles in Figure S6) and (*ii*) from the linear fitting for the E_{tot}^{slab} with respect to N (indicated by squares in Figure S6).

The work function, Φ, was calculated using Equation S2:

$$\Phi = V_{es}(\mathbf{r}_{vac}) - \epsilon_{\mathrm{F}} \ , \tag{S2}$$

where $V_{es}(\mathbf{r}_{vac})$ is the electrostatic potential in the vacuum and ϵ_{F} is the Fermi energy.

The interlayer relaxation, in percentage, compared with the ideal (bulk equillibrium positions) surface, Δd_{ij}, was calculated, with respect to layers i and j, as shown in Equation S3:

$$\Delta d_{ij} = \frac{(d_{ij} - d_0)\times 100}{d_0} \ , \tag{S3}$$

where d_{ij} is the interlayer spacing for the relaxed surface, d_0 is the interlayer spacing in the ideal surface.

Figure S7 shows the total density of states for the top and center layers of undoped Pt(100)-1x1 slabs with N layers.

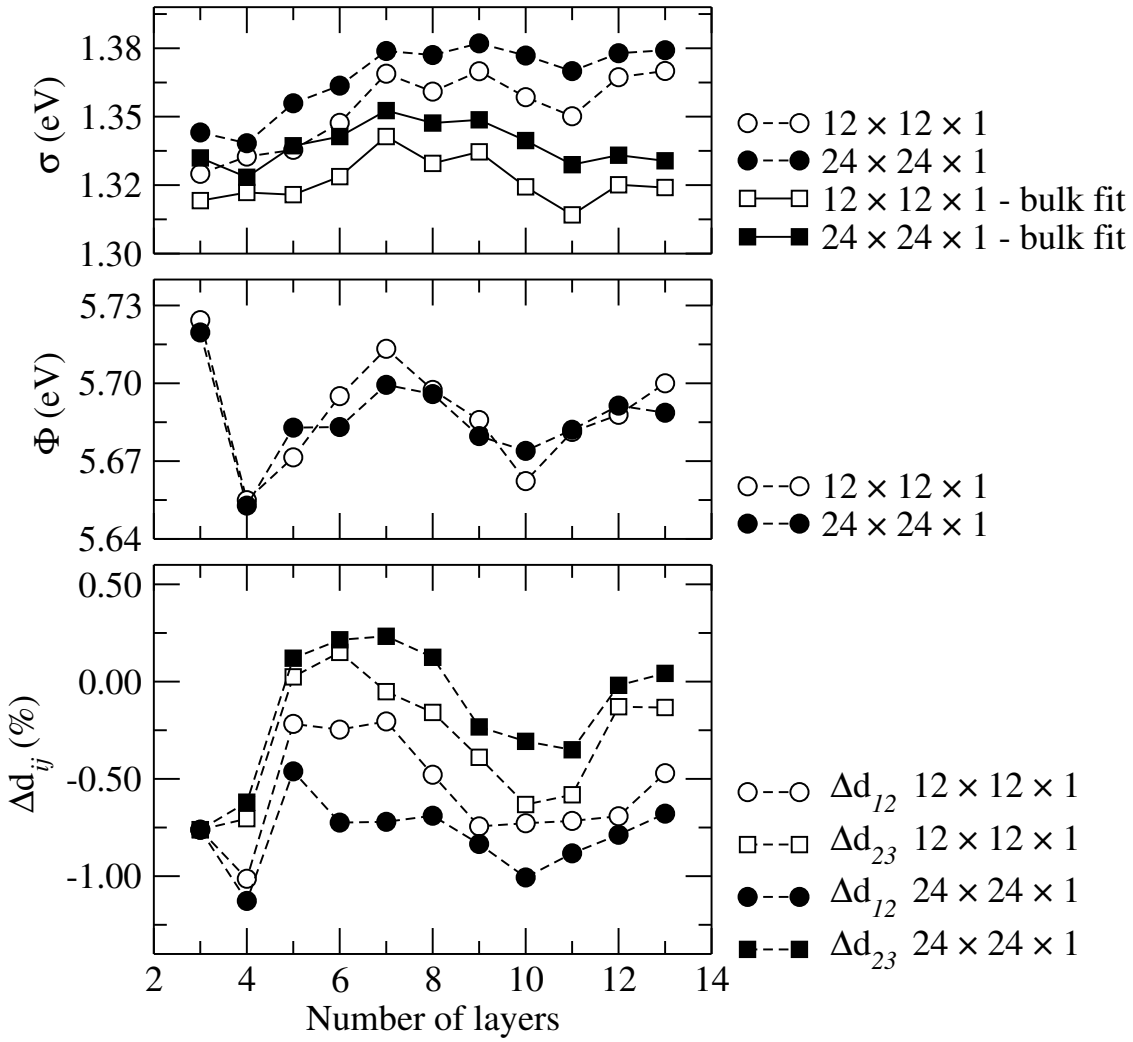

Figure S6: Surface energy σ, work function Φ and interlayer spacing Δd_{ij} as functions of the number of layers using the $12\times12\times1$ (open circles and squares) and $24\times24\times1$ (closed circles and squares) k-points meshes for the Pt(100) slab.

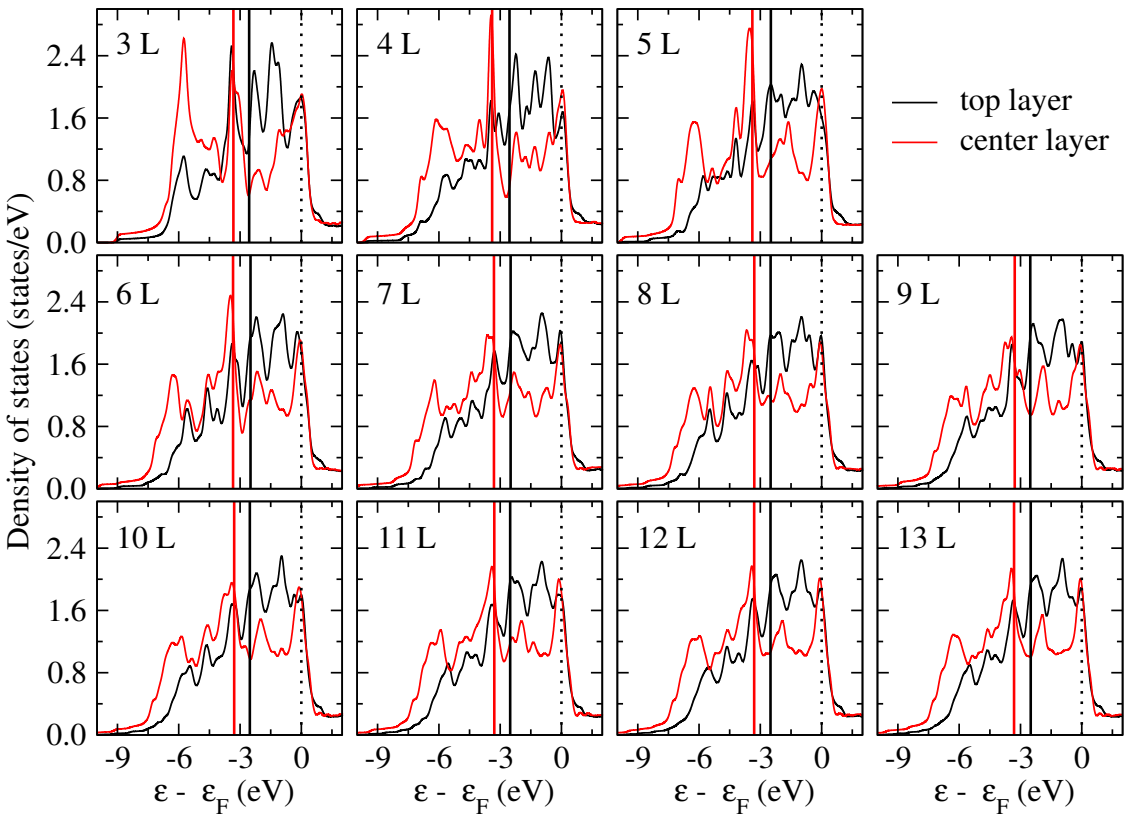

Figure S7: Density of states for the top and center layers of the Pt(100)-1×1 slab with N layers. The vertical solid lines indicates the *d*-band center for the respective layers and the dashed line indicates the Fermi level energy.

6 Doped Pt(100) Substrates

Figure S8 shows 3×3 Pt(100) slabs indicating positions where the Pt was substituted by a TM for the example of the Fe dopant; other dopants followed the same pattern. The energetic and magnetic properties of the doped Pt(100) substrates with the TM atoms in the three topmost layers are displayed in the Table S2. In Table S3, we show the structural properties of the doped Pt(100) substrates, such as effective coordination number (ECN), in units of number of nearest neighbors (NNN), and average bond length (d_{av}), in Å. The

ECN_i (for each atom i) were calculated as

$$\mathrm{ECN}_i = \sum_{\substack{j=1,\\ i\neq j}}^{N} w_{ij} = \sum_{\substack{j=1,\\ i\neq j}}^{N} exp\left[1 - \left(\frac{d_{ij}}{(d_{av}^{i} + d_{av}^{j})/2}\right)^{6}\right] , \tag{S4}$$

and the average d_{av}^{i} (for each atom)

$$d_{av}^{i} = \frac{\sum_{\substack{j=1,\\ i\neq j}}^{N} d_{ij} exp\left[1 - \left(\frac{d_{ij}}{(d_{av}^{i}+d_{av}^{j})/2}\right)^{6}\right]}{\sum_{\substack{j=1,\\ i\neq j}}^{N} exp\left[1 - \left(\frac{d_{ij}}{(d_{av}^{i}+d_{av}^{j})/2}\right)^{6}\right]}. \tag{S5}$$

We obtained the ECN of the atoms per layer i, $\mathrm{ECN}_{\mathrm{Pt\text{-}Li}}$, as the average ECN considering all atoms of the layer. The same was made for $d_{av}^{\mathrm{Pt\text{-}Li}}$.

The local density of states for the topmost layer of the clean undoped and doped substrates are shown in Figure S9. To calculate the average d-band center ε_d for each layer, we taking the average value between the d-band center of the up and down bands for the specific layer using the equation:

$$\varepsilon_d = (\varepsilon_d^{up} + \varepsilon_d^{down})/2. \tag{S6}$$

The Table S4 displays the d-band centers of the undoped Pt(100) for topmost layers (1 and 2) and the d-band centers up and down bands in the layers 1 and 2 and the average among these bands for each layer of the doped substrates. Figures S10 and S11 show the charge in the two topmost layers in the undoped and doped substrates. And the Table S5 contains the charge on the TM atom, Q_{eff}^{TM}; the average charge on surface Pt atoms, $Q_{eff}^{Pt(sur)}$; the average charge on subsurface Pt atoms, $Q_{eff}^{Pt(sub)}$; the sum of the charges for the surface layer, Q_{eff}^{sur} and the sum of the charges for the subsurface layer, Q_{eff}^{sub} in e.

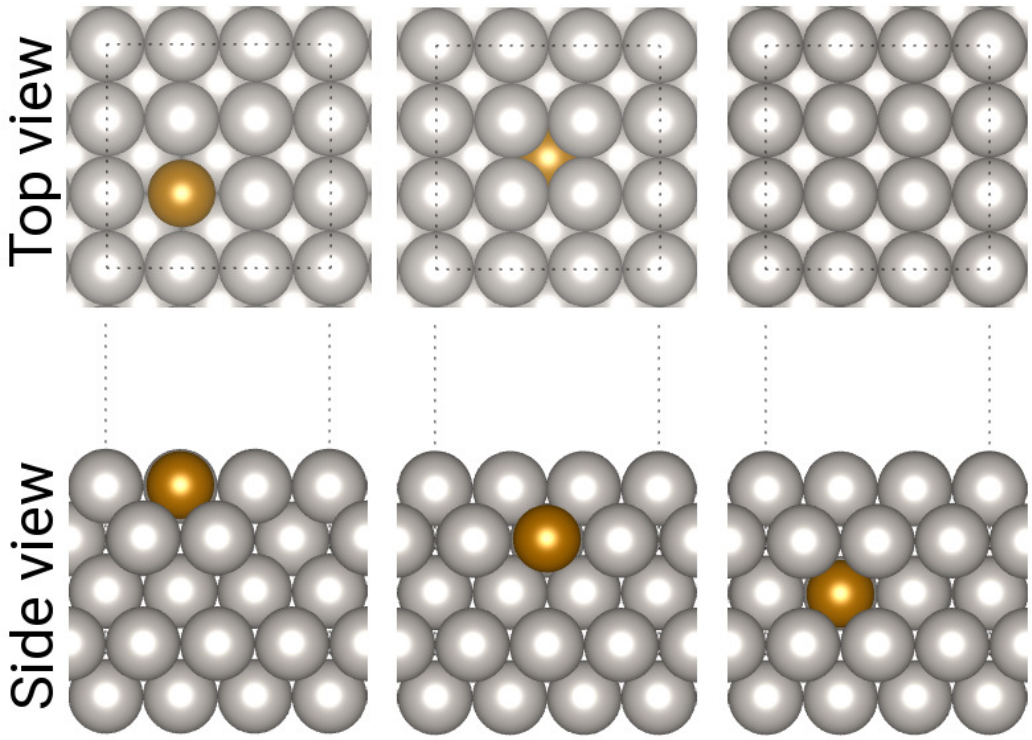

Figure S8: Configurations for clean PtFe(100) surface illustrating three positions studied for the TM dopants.

Table S2: Total energies, E_{tot} (in eV), relative energies, ΔE_{tot} (in eV), with respect to the Pt_8TM_1/Pt(100) configuration (i.e., in which the TM is on the surface for each PtTM(100)), total, m_{tot}, and local, m_{loc}^{TM}, magnetic moments (in μ_B) for the clean surfaces.

System	E_{tot} (eV)	ΔE_{tot} (eV)	m_{tot} (μ_B)	m_{loc}^{TM} (μ_B)
$Pt_9/Pt_8Fe_1/Pt_9/Pt(100)$	−288.472 298 54	−0.63	4.44	3.26
$Pt_9/Pt_9/Pt_8Fe_1/Pt(100)$	−288.422 854 11	−0.58	4.22	3.21
$Pt_8Fe_1/Pt_9/Pt_9/Pt(100)$	−287.842 768 92	0.00	3.39	3.31
$Pt_9/Pt_9/Pt_8Co_1/Pt(100)$	−286.615 938 37	−0.63	3.34	2.11
$Pt_9/Pt_8Co_1/Pt_9/Pt(100)$	−286.594 378 06	−0.61	2.96	2.09
$Pt_8Co_1/Pt_9/Pt_9/Pt(100)$	−285.987 750 16	0.00	2.10	2.09
$Pt_9/Pt_8Ni_1/Pt_9/Pt(100)$	−285.041 366 56	−0.48	0.83	0.75
$Pt_9/Pt_9/Pt_8Ni_1/Pt(100)$	−284.984 584 79	−0.42	1.00	0.75
$Pt_8Ni_1/Pt_9/Pt_9/Pt(100)$	−284.563 726 90	0.00	0.13	0.40
$Pt_9/Pt_9/Pt_8Ru_1/Pt(100)$	−288.448 114 33	−0.79	0.00	0.00
$Pt_9/Pt_8Ru_1/Pt_9/Pt(100)$	−287.654 526 41	−0.69	1.82	0.49
$Pt_8Ru_1/Pt_9/Pt_9/Pt(100)$	−284.670 765 14	0.00	2.17	1.54
$Pt_9/Pt_9/Pt_8Rh_1/Pt(100)$	−286.538 080 53	−0.41	0.56	0.15
$Pt_9/Pt_8Rh_1/Pt_9/Pt(100)$	−286.532 148 42	−0.40	0.43	0.02
$Pt_8Rh_1/Pt_9/Pt_9/Pt(100)$	−286.132 826 61	0.00	1.12	0.32
$Pt_9/Pt_9/Pt_8Pd_1/Pt(100)$	−284.535 945 74	0.13	0.05	0.00
$Pt_9/Pt_8Pd_1/Pt_9/Pt(100)$	−284.570 597 23	0.10	0.00	0.00
$Pt_8Pd_1/Pt_9/Pt_9/Pt(100)$	−284.670 765 14	0.00	0.18	0.00

Table S3: Average effective coordination number (NNN) and average weighted bond length (Å), for the Pt atoms in the three topmost layers ($\mathbf{ECN_{Pt\text{-}L1}}$, $d_{av}^{\mathbf{Pt\text{-}L1}}$; $\mathbf{ECN_{Pt\text{-}L2}}$, $d_{av}^{\mathbf{Pt\text{-}L2}}$; $\mathbf{ECN_{Pt\text{-}L3}}$ and $d_{av}^{\mathbf{Pt\text{-}L3}}$) and for the TM atom ($\mathbf{ECN_{TM}}$ and $d_{av}^{\mathbf{TM}}$) in the clean surfaces.

System	$ECN_{Pt\text{-}L1}$	$d_{av}^{Pt\text{-}L1}$ (Å)	$ECN_{Pt\text{-}L2}$	$d_{av}^{Pt\text{-}L2}$ (Å)	$ECN_{Pt\text{-}L3}$	$d_{av}^{Pt\text{-}L3}$ (Å)	ECN_{TM}	d_{av}^{TM} (Å)
Pt(100)	8.02	2.77	12.02	2.77	12.01	2.77	-	-
$Pt_9/Pt_8Fe_1/Pt_9/Pt(100)$	7.99	2.75	11.97	2.76	11.97	2.76	12.34	2.72
$Pt_9/Pt_9/Pt_8Fe_1/Pt(100)$	7.98	2.77	12.00	2.76	12.00	2.76	12.34	2.73
$Pt_8Fe_1/Pt_9/Pt_9/Pt(100)$	8.03	2.76	12.01	2.77	11.99	2.77	7.93	2.77
$Pt_9/Pt_9/Pt_8Co_1/Pt(100)$	7.98	2.77	12.00	2.76	12.00	2.76	12.35	2.73
$Pt_9/Pt_8Co_1/Pt_9/Pt(100)$	7.98	2.75	11.99	2.76	11.98	2.76	12.37	2.72
$Pt_8Co_1/Pt_9/Pt_9/Pt(100)$	7.99	2.76	12.00	2.76	11.97	2.77	8.25	2.71
$Pt_9/Pt_8Ni_1/Pt_9/Pt(100)$	7.98	2.75	11.99	2.76	12.00	2.76	12.37	2.72
$Pt_9/Pt_9/Pt_8Ni_1/Pt(100)$	7.98	2.77	12.00	2.76	12.01	2.76	12.31	2.73
$Pt_8Ni_1/Pt_9/Pt_9/Pt(100)$	7.96	2.76	12.01	2.76	11.97	2.77	8.44	2.69
$Pt_9/Pt_9/Pt_8Ru_1/Pt(100)$	8.00	2.77	12.01	2.76	11.99	2.76	12.24	2.74
$Pt_9/Pt_8Ru_1/Pt_9/Pt(100)$	8.00	2.76	12.01	2.76	11.99	2.76	12.25	2.74
$Pt_8Ru_1/Pt_9/Pt_9/Pt(100)$	7.96	2.77	12.01	2.76	11.98	2.77	8.45	2.71
$Pt_9/Pt_9/Pt_8Rh_1/Pt(100)$	8.01	2.77	12.02	2.76	12.01	2.77	12.13	2.75
$Pt_9/Pt_8Rh_1/Pt_9/Pt(100)$	8.01	2.76	12.02	2.76	12.01	2.76	12.16	2.75
$Pt_8Rh_1/Pt_9/Pt_9/Pt(100)$	7.99	2.76	12.02	2.76	11.99	2.77	8.23	2.73
$Pt_9/Pt_9/Pt_8Pd_1/Pt(100)$	8.01	2.77	12.02	2.77	12.01	2.77	12.05	2.76
$Pt_9/Pt_8Pd_1/Pt_9/Pt(100)$	8.02	2.77	12.02	2.77	12.01	2.77	12.07	2.76
$Pt_8Pd_1/Pt_9/Pt_9/Pt(100)$	8.05	2.76	12.02	2.77	12.00	2.77	7.72	2.80

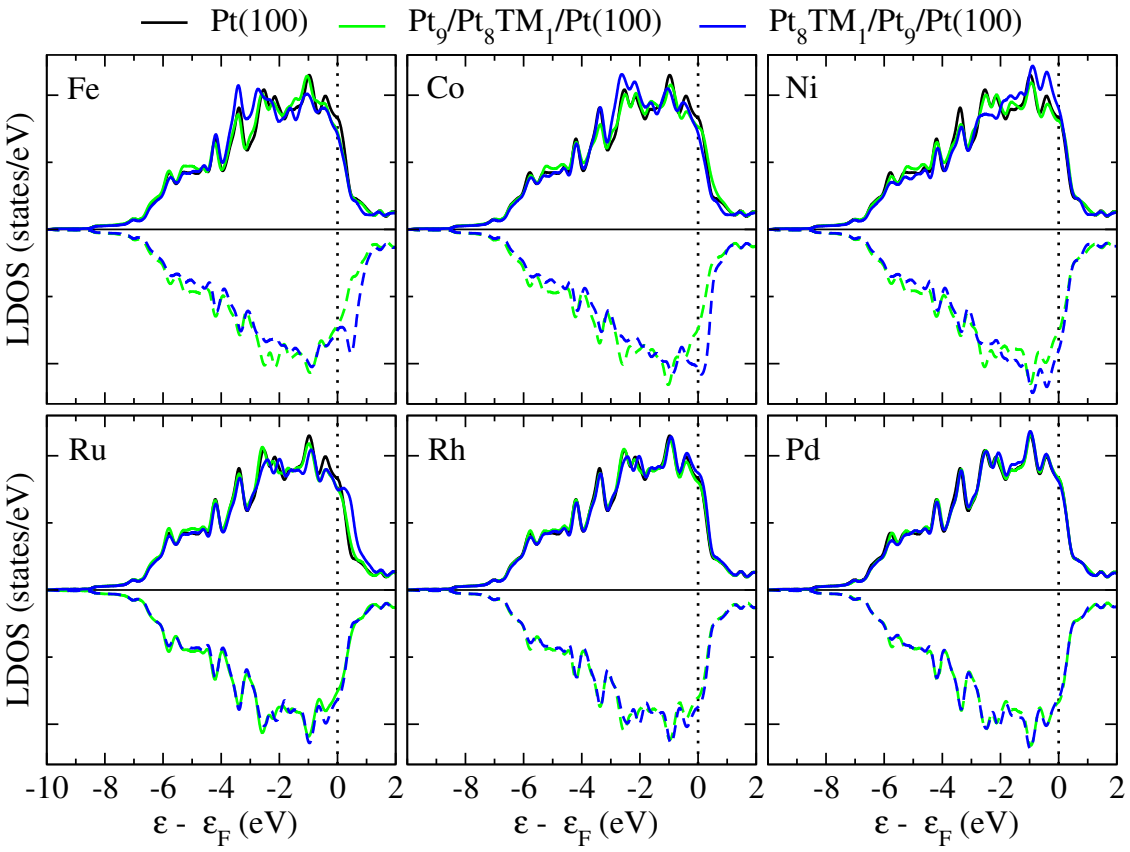

Figure S9: Local density of states (LDOS) for the topmost layer of the clean Pt(100), $Pt_9/Pt_8TM_1/Pt(100)$ and $Pt_8TM_1/Pt_9/Pt(100)$ surfaces. For Pt(100), the LDOS curve of the topmost layer is divided by 2 because is a no spin polarization calculation. The vertical dashed lines indicate the Fermi level.

Table S4: The d-band center for the two topmost layers (1 and 2), ε_d^i, taken as the average between the up and down bands, $\varepsilon_d^{up(i)}$ and $\varepsilon_d^{down(i)}$.

Substrate	$\varepsilon_d^{up(1)}$	$\varepsilon_d^{down(1)}$	ε_d^1	$\varepsilon_d^{up(2)}$	$\varepsilon_d^{down(2)}$	ε_d^2
Pt(100)			−2.50			−3.31
$Pt_9/Pt_8Fe_1/Pt_9/Pt(100)$	−2.5333	−2.5382	−2.54	−3.3313	−3.3139	−3.32
$Pt_8Fe_1/Pt_9/Pt_9/Pt(100)$	−2.5695	−2.4478	−2.51	−3.2887	−3.3052	−3.30
$Pt_9/Pt_8Co_1/Pt_9/Pt(100)$	−2.5298	−2.5266	−2.53	−3.2312	−3.2662	−3.25
$Pt_8Co_1/Pt_9/Pt_9/Pt(100)$	−2.4918	−2.3880	−2.44	−3.3067	−3.3290	−3.32
$Pt_9/Pt_8Ni_1/Pt_9/Pt(100)$	−2.5098	−2.5093	−2.51	−3.1417	−3.1645	−3.15
$Pt_8Ni_1/Pt_9/Pt_9/Pt(100)$	−2.3374	−2.3374	−2.34	−3.3203	−3.3203	−3.32
$Pt_9/Pt_8Ru_1/Pt_9/Pt(100)$	−2.5558	−2.5558	−2.56	−3.3240	−3.3226	−3.32
$Pt_8Ru_1/Pt_9/Pt_9/Pt(100)$	−2.5079	−2.5028	−2.51	−3.3584	−3.3487	−3.35
$Pt_9/Pt_8Rh_1/Pt_9/Pt(100)$	−2.5143	−2.5143	−2.51	−3.2754	−3.2754	−3.28
$Pt_8Rh_1/Pt_9/Pt_9/Pt(100)$	−2.4545	−2.4545	−2.45	−3.3311	−3.3311	−3.33
$Pt_9/Pt_8Pd_1/Pt_9/Pt(100)$	−2.4742	−2.4742	−2.47	−3.2371	−3.2371	−3.24
$Pt_8Pd_1/Pt_9/Pt_9/Pt(100)$	−2.4560	−2.4560	−2.46	−3.2995	−3.2995	−3.30

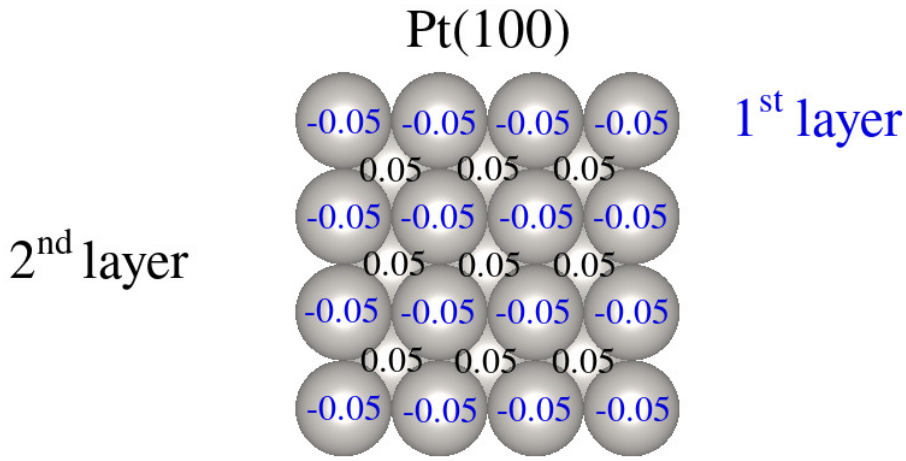

Figure S10: Top view of the Pt(100) surface showing the effective Bader charges of each atom for the two topmost layers of the Pt(100) slab.

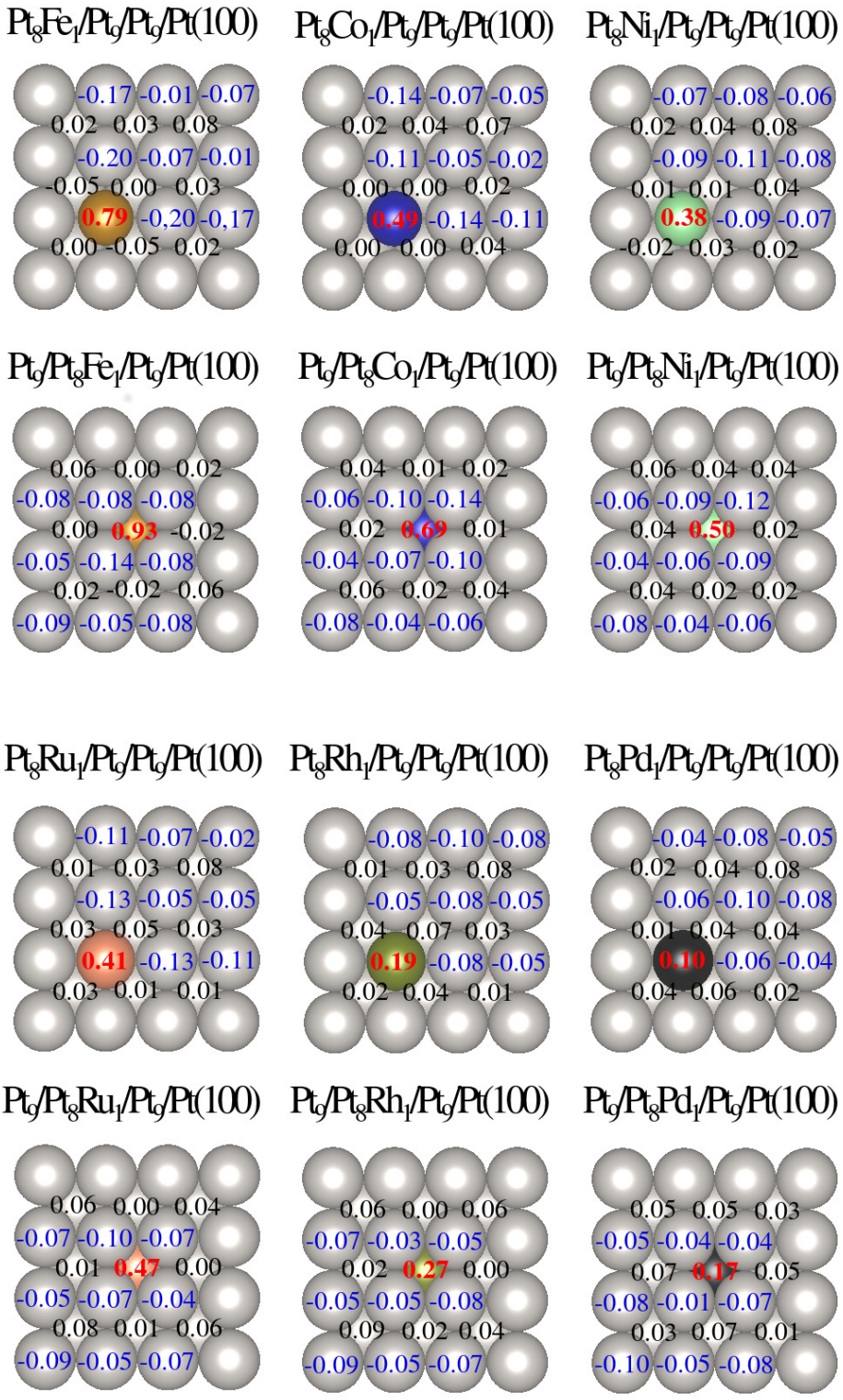

Figure S11: Top view of the surface slabs showing the effective charges for the clean $Pt_9/Pt_8TM_1/Pt(100)$ and $Pt_8TM_1/Pt_9/Pt(100)$ surface and subsurface layers.

Table S5: Effective charges for the clean surfaces, in e: the charge on the TM atom, Q_{eff}^{TM}; the average charge on surface Pt atoms, $Q_{eff}^{Pt(sur)}$; the average charge on subsurface Pt atoms, $Q_{eff}^{Pt(sub)}$; the sum of the charges for the surface layer, Q_{eff}^{sur} and the sum of the charges for the subsurface layer, Q_{eff}^{sub}.

Substrate	Q_{eff}^{TM}	$Q_{eff}^{Pt(sur)}$	$Q_{eff}^{Pt(sub)}$	Q_{eff}^{sur}	Q_{eff}^{sub}
			e		
Pt(100)		−0.05	0.05	−0.47	0.41
$Pt_9/Pt_8Fe_1/Pt_9/Pt(100)$	0.93	−0.09	0.01	−0.80	1.04
$Pt_8Fe_1/Pt_9/Pt_9/Pt(100)$	0.79	−0.11	0.01	−0.10	0.06
$Pt_9/Pt_8Co_1/Pt_9/Pt(100)$	0.69	−0.08	0.03	−0.71	0.89
$Pt_8Co_1/Pt_9/Pt_9/Pt(100)$	0.46	−0.09	0.02	−0.22	0.19
$Pt_9/Pt_8Ni_1/Pt_9/Pt(100)$	0.50	−0.07	0.03	−0.64	0.76
$Pt_8Ni_1/Pt_9/Pt_9/Pt(100)$	0.38	−0.08	0.02	−0.25	0.21
$Pt_9/Pt_8Ru_1/Pt_9/Pt(100)$	0.47	−0.07	0.03	−0.62	0.73
$Pt_8Ru_1/Pt_9/Pt_9/Pt(100)$	0.41	−0.08	0.03	−0.26	0.25
$Pt_9/Pt_8Rh_1/Pt_9/Pt(100)$	0.27	−0.06	0.04	−0.56	0.58
$Pt_8Rh_1/Pt_9/Pt_9/Pt(100)$	0.19	−0.07	0.04	−0.37	0.33
$Pt_9/Pt_8Pd_1/Pt_9/Pt(100)$	0.17	−0.06	0.04	−0.52	0.51
$Pt_8Pd_1/Pt_9/Pt_9/Pt(100)$	0.10	−0.06	0.04	−0.40	0.34

7 Additional Results for the Adsorption of Ethylene Glycol on Undoped and Doped Pt(100) Substrates

All adsorption configurations studied for the adsorption of ethylene glycol on undoped and doped Pt(100) substrates are shown in Figures S12, S13, S14, S15, S16, S17, S18 along with the relative total energies, with respect to the lowest energy configuration within the set, for all systems.

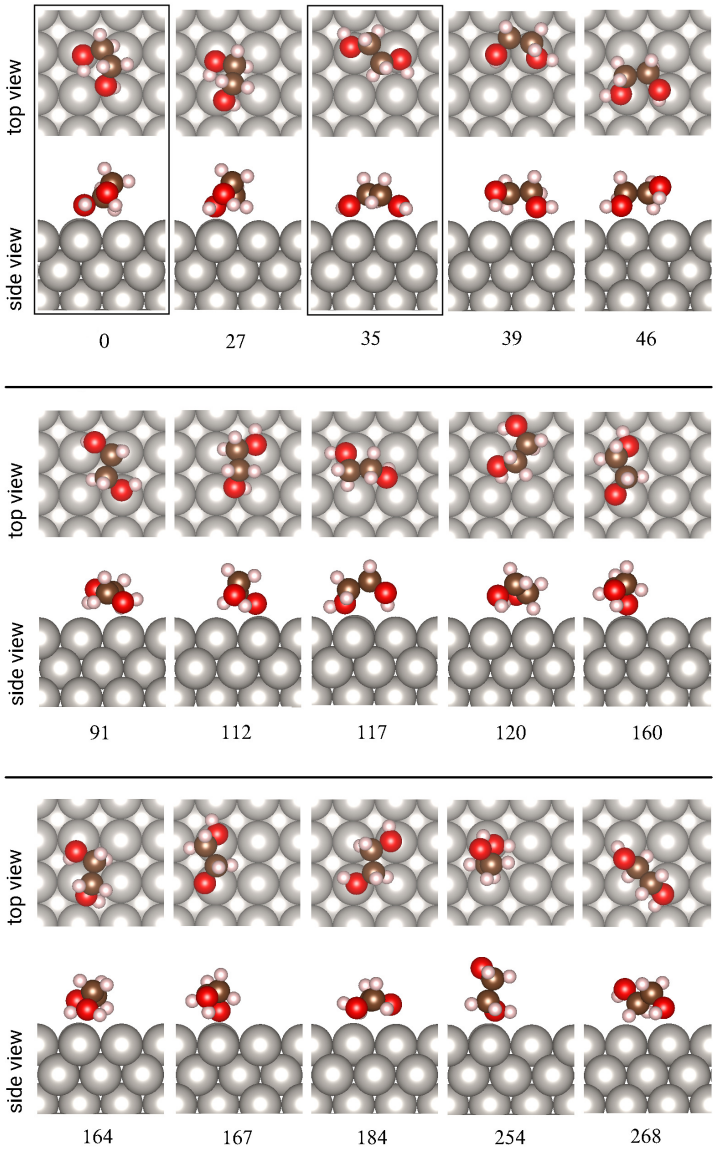

Figure S12: EG/Pt(100) configurations and their relative energies in meV with respect to the lowest energy configuration.

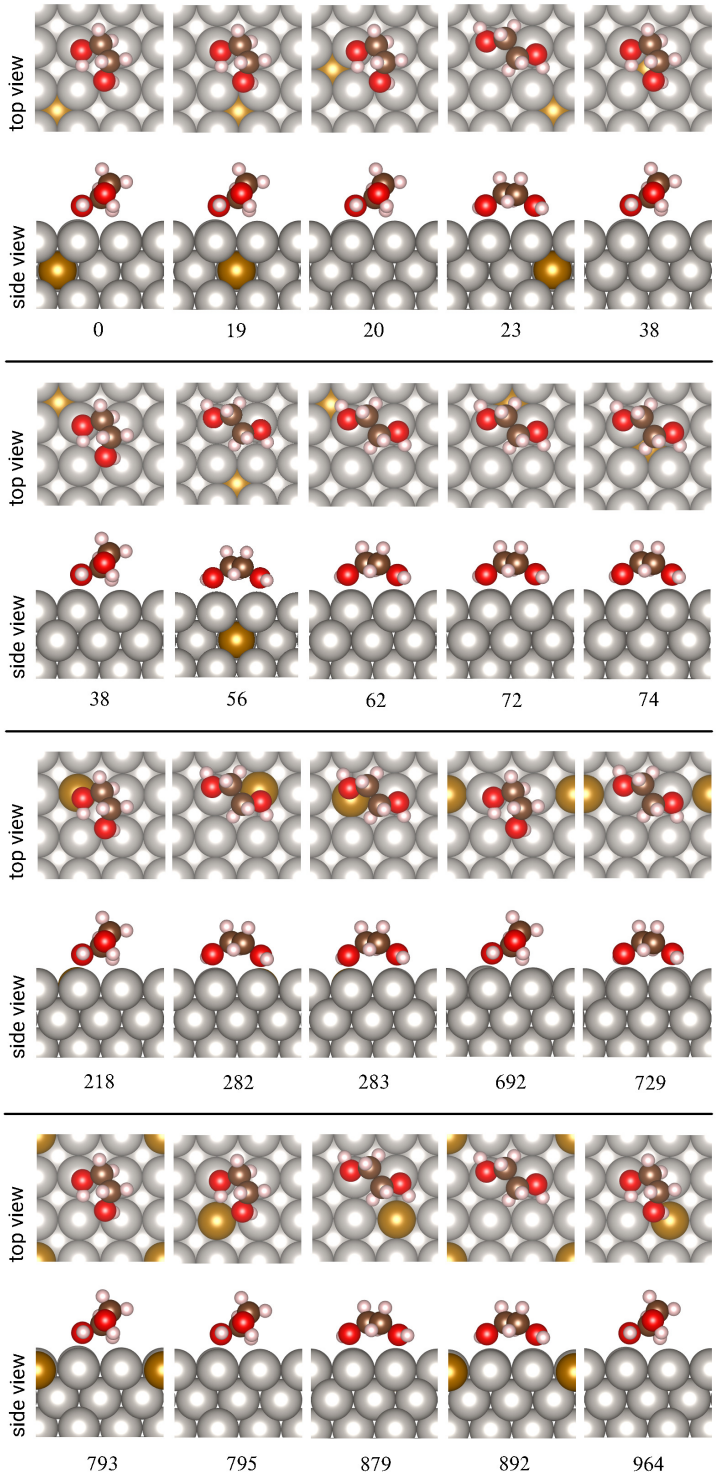

Figure S13: EG/Pt_9/Pt_8Fe_1/Pt(100) and EG/Pt_8Fe_1/Pt_9/Pt(100) configurations and their relative energies (meV) with respect to the lowest energy configuration.

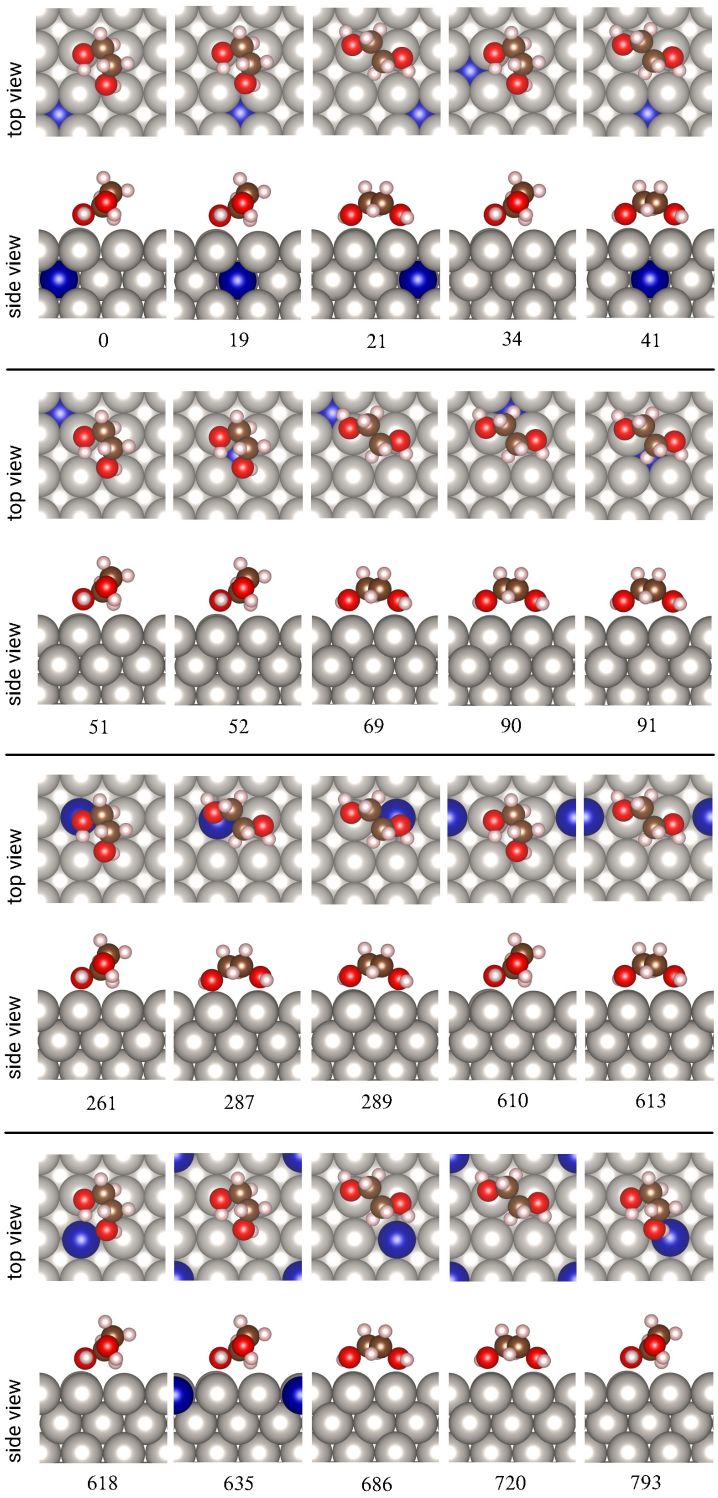

Figure S14: EG/Pt_9/Pt_8Co_1/Pt(100) and EG/Pt_8Co_1/Pt_9/Pt(100) configurations and their relative energies (meV) with respect to the lowest energy configuration.

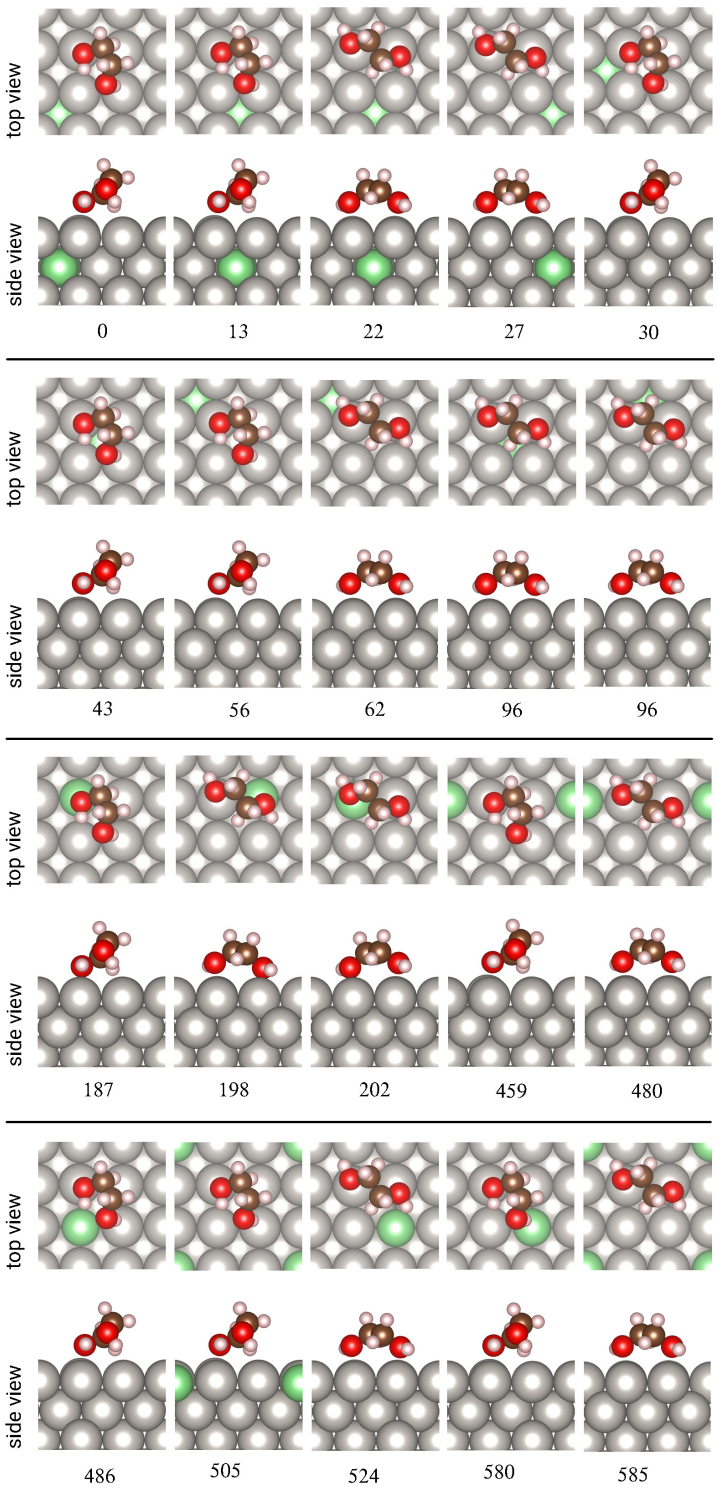

Figure S15: EG/Pt_9/Pt_8Ni_1/Pt(100) and EG/Pt_8Ni_1/Pt_9/Pt(100) configurations and their relative energies (meV) with respect to the lowest energy configuration.

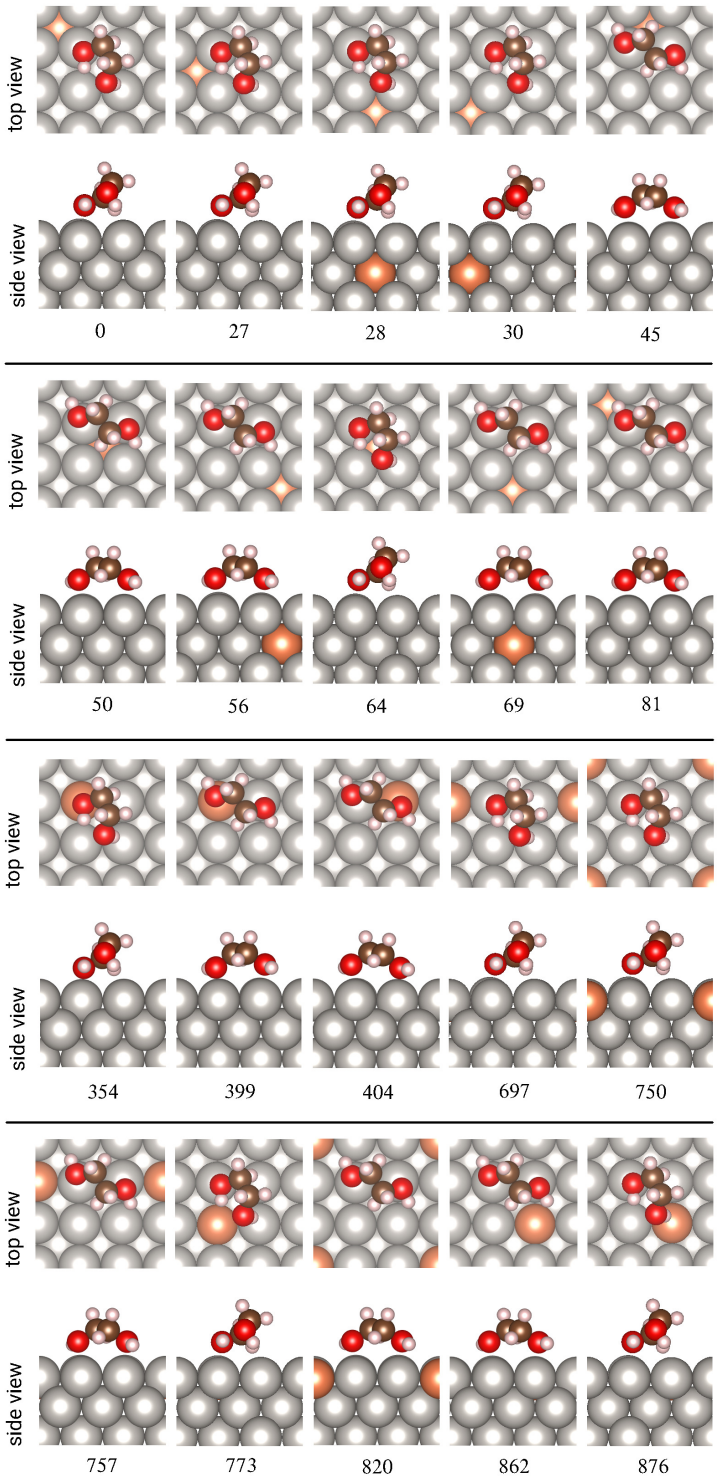

Figure S16: EG/Pt_9/Pt_8Ru_1/Pt(100) and EG/Pt_8Ru_1/Pt_9/Pt(100) configurations and their relative energies (meV) with respect to the lowest energy configuration.

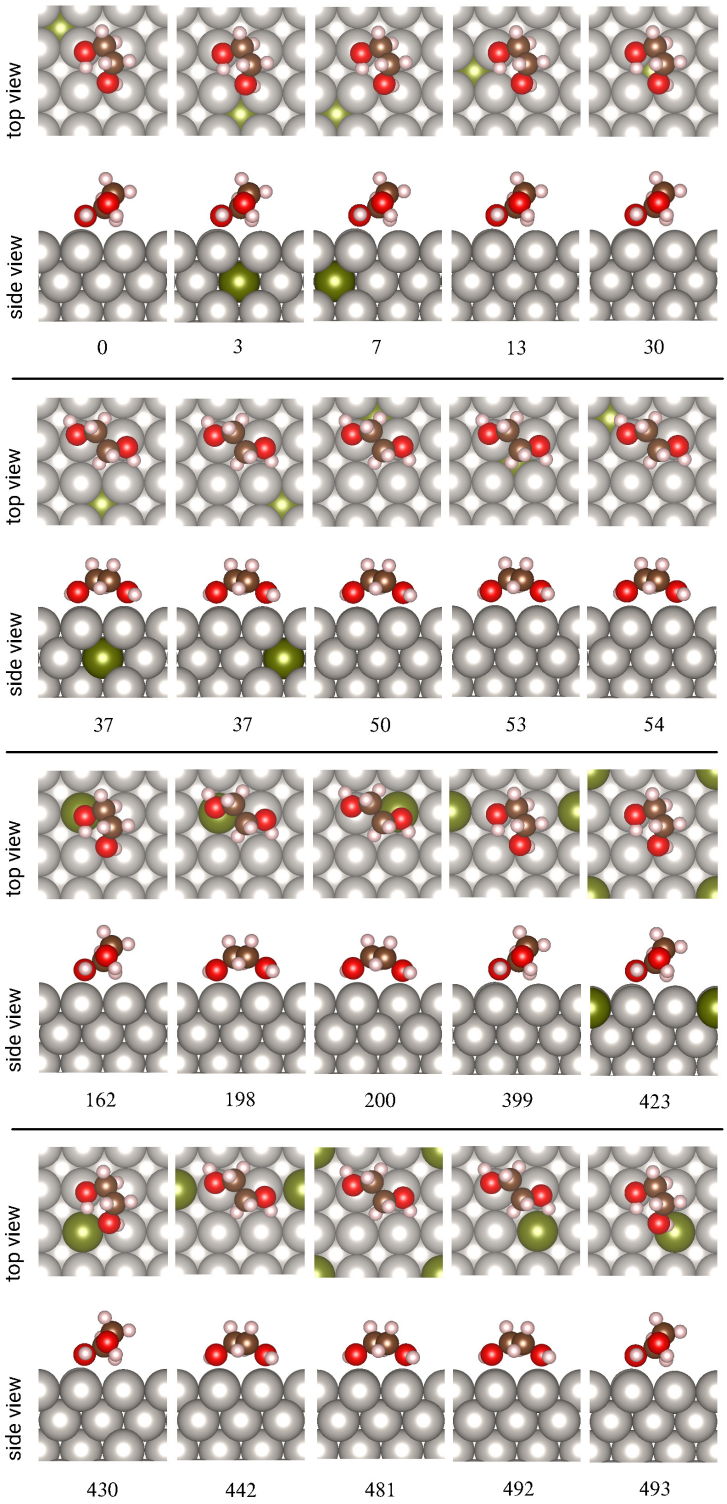

Figure S17: EG/Pt_9/Pt_8Rh_1/Pt(100) and EG/Pt_8Rh_1/Pt_9/Pt(100) configurations and their relative energies (meV) with respect to the lowest energy configuration.

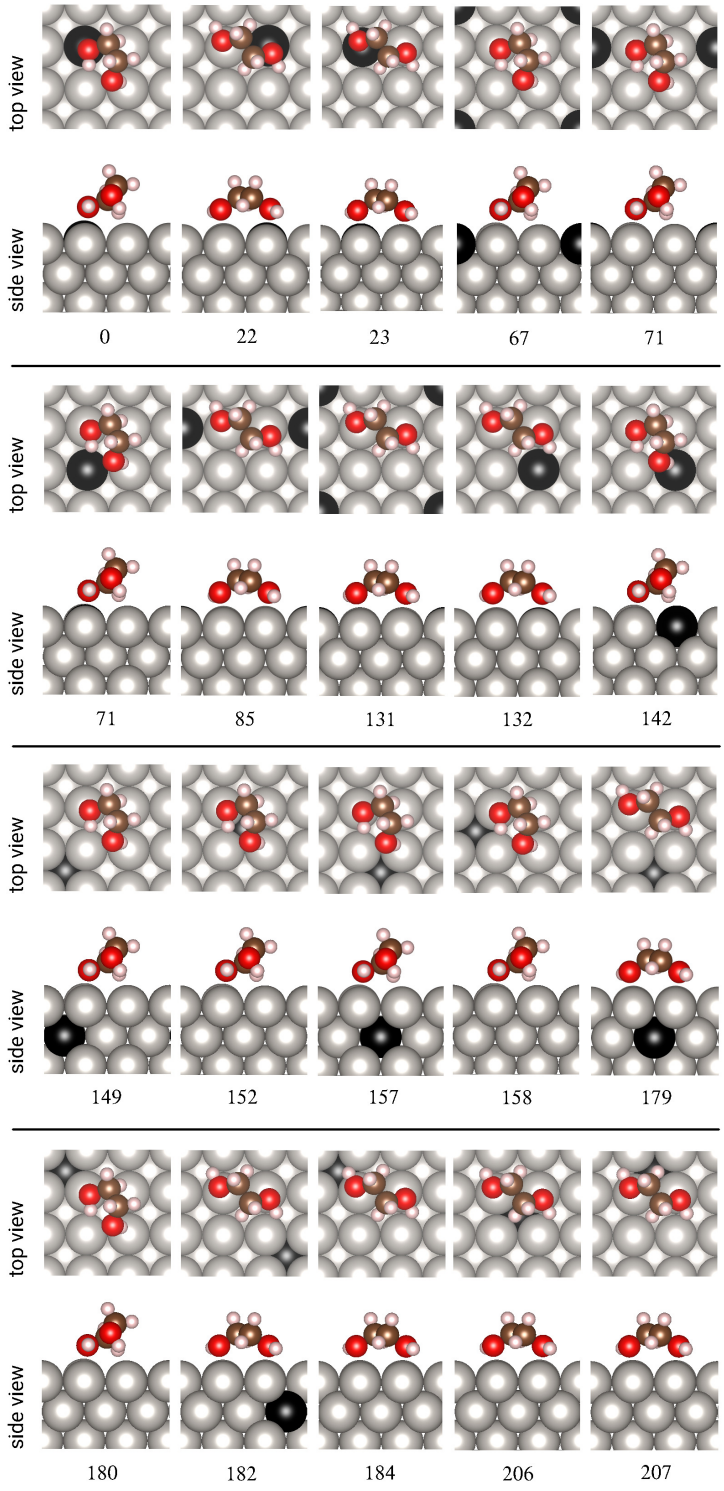

Figure S18: EG/Pt_9/Pt_8Pd_1/Pt(100) and EG/Pt_8Pd_1/Pt_9/Pt(100) configurations and their relative energies (meV) with respect to the lowest energy configuration.

8 Effect of the dipole correction in the adsorbed systems

To demonstrate the effect of the dipole correction on the total energy and magnetic moments of the adsorbed systems, Table **??** shows some results for ethylene glycol adsorbed on doped surfaces without and with the dipole correction. As expected, the effects on the total energy are very small (within 10 meV), hence, the correction was employed only to calculate the work functions, as explained in the main article.

Table S6: Total energy,E_{tot}, and magnetic moment, m_{tot}, for the lowest energy configurations of the adsorbed doped systems without and with dipole correction and the difference in the total energy due to the dipole correction, ΔE_{tot}.

Configuration	E_{tot} (meV)	m_{tot} (μ_B)	E_{tot} (meV)	m_{tot} (μ_B)	ΔE_{tot}
	No Dipole Correction		Dipole Correction		
$EG^{1O}/Pt_9/Pt_8Fe_1$	-342.93623857	4.5387	-342.92309795	4.5394	-0.01314062
$EG^{1O}/Pt_9/Pt_8Co_1$	-341.07952862	2.6842	-341.06635930	2.6803	-0.01316932
$EG^{1O}/Pt_9/Pt_8Ni_1$	-339.52658504	1.5473	-339.51371433	1.5490	-0.01287071
$EG^{1O}/Pt_9/Pt_8Ru_1$	-342.85404760	0.8631	-342.84198283	0.8764	-0.01206477
$EG^{1O}/Pt_9/Pt_8Rh_1$	-341.02312774	0.5785	-341.01133282	0.5866	-0.01179492
$EG^{1O}/Pt_8Pd_1/Pt_9$	-339.19678195	0.3550	-339.18734907	0.3476	-0.00943288

9 Geometric properties of adsorbed systems: bond lengths and angles

In Table S7, we show percent variations in the bond lengths of the molecule, due to adsorption. Furthermore, we provide the distances between C, O and H atoms to the metal atom on the surface of the substrates.

Table S8 shows the $\alpha_{CC\perp}$ angle as well as the changes in the main bond angles and dihedral.

Table S7: Percent variations, with respect to gas-phase ethylene glycol, in the C−C, C−O and O−H bond lengths, due to the adsorption on the undoped and doped substrates. Shortest distances between the C, O and H atoms and a metal atom on surface of the substrate, as well as the perpendicular distances between the C, O and H atoms and the surface plane.

System/Pt(100)	$\Delta d_{C_1-C_2}$ (%)	$\Delta d_{C_1-O_1}$ (%)	$\Delta d_{C_2-O_2}$ (%)	$\Delta d_{O_1-H_1}$ (%)	$\Delta d_{O_2-H_2}$ (%)	d_{C_1-Pt} (Å)	d_{C_2-Pt} (Å)	d_{O_1-Pt} (Å)	d_{O_2-Pt} (Å)	$d^{\perp}_{C_1-Pt}$ (Å)	$d^{\perp}_{C_2-Pt}$ (Å)	$d^{\perp}_{O_1-Pt}$ (Å)	$d^{\perp}_{O_2-Pt}$ (Å)
EG^{2O}	0.53	1.40	1.36	1.33	1.48	3.27	3.27	2.35	2.36	3.11	3.08	2.35	2.36
EG^{1O}	0.45	1.70	−0.51	2.11	1.97	3.21	3.98	2.27	3.40	2.90	3.77	2.35	3.17
$EG^{2O}/Pt_8Fe_1/Pt_9$	0.35	1.64	1.33	2.25	1.75	3.23	3.29	2.20	2.34	3.04	3.09	2.21	2.32
$EG^{1O}/Pt_8Fe_1/Pt_9$	0.45	1.88	−0.53	2.41	2.16	3.09	3.95	2.13	3.38	2.82	3.70	2.26	3.13
$EG^{2O}/Pt_9/Pt_8Fe_1$	0.49	1.53	1.32	1.35	1.50	3.26	3.29	2.32	2.37	3.12	3.09	2.35	2.35
$EG^{1O}/Pt_9/Pt_8Fe_1$	0.43	1.60	−0.45	1.97	1.92	3.23	3.97	2.30	3.42	2.92	3.79	2.36	3.19
$EG^{2O}/Pt_8Co_1/Pt_9$	0.30	1.51	1.41	1.92	1.77	3.17	3.26	2.14	2.32	3.00	3.04	2.11	2.31
$EG^{1O}/Pt_8Co_1/Pt_9$	0.35	1.42	−0.64	2.03	2.14	3.06	3.94	2.12	3.39	2.75	3.68	2.16	3.12
$EG^{2O}/Pt_9/Pt_8Co_1$	0.45	1.59	1.35	1.43	1.55	3.25	3.28	2.32	2.36	3.12	3.09	2.35	2.34
$EG^{1O}/Pt_9/Pt_8Co_1$	0.47	1.64	−0.47	2.01	1.96	3.22	3.97	2.28	3.41	2.92	3.79	2.36	3.18
$EG^{2O}/Pt_8Ni_1/Pt_9$	0.19	1.69	1.37	2.05	1.72	3.09	3.25	2.05	2.33	2.91	3.03	1.98	2.32
$EG^{1O}/Pt_8Ni_1/Pt_9$	0.37	1.42	−0.68	2.18	2.14	3.01	3.90	2.04	3.38	2.69	3.64	2.06	3.08
$EG^{2O}/Pt_9/Pt_8Ni_1$	0.44	1.41	1.38	1.40	1.56	3.27	3.27	2.34	2.34	3.12	3.09	2.34	2.33
$EG^{1O}/Pt_9/Pt_8Ni_1$	0.45	1.71	−0.48	2.09	1.96	3.21	3.98	2.27	3.41	2.92	3.79	2.35	3.19
$EG^{2O}/Pt_8Ru_1/Pt_9$	0.22	1.97	1.34	1.76	1.91	3.26	3.22	2.21	2.35	3.00	3.05	2.11	2.31
$EG^{1O}/Pt_8Ru_1/Pt_9$	0.76	2.19	−0.51	2.70	2.24	3.16	3.96	2.17	3.38	2.81	3.70	2.13	3.10
$EG^{2O}/Pt_9/Pt_8Ru_1$	0.54	1.44	1.41	1.49	1.28	3.28	3.29	2.38	2.39	3.10	3.13	2.35	2.38
$EG^{1O}/Pt_9/Pt_8Ru_1$	0.50	1.67	−0.53	2.04	2.05	3.23	3.99	2.29	3.39	2.91	3.78	2.35	3.19
$EG^{2O}/Pt_8Rh_1/Pt_9$	0.33	1.76	1.34	1.58	1.76	3.22	3.25	2.21	2.36	3.04	3.06	2.20	2.33
$EG^{1O}/Pt_8Rh_1/Pt_9$	0.61	1.86	−0.53	2.31	2.12	3.15	3.96	2.18	3.38	2.84	3.72	2.21	3.13
$EG^{2O}/Pt_9/Pt_8Rh_1$	0.50	1.44	1.42	1.28	1.44	3.28	3.27	2.35	2.35	3.13	3.10	2.36	2.35
$EG^{1O}/Pt_9/Pt_8Rh_1$	0.46	1.73	−0.51	2.06	2.01	3.22	3.98	2.27	3.39	2.91	3.78	2.35	3.18
$EG^{2O}/Pt_8Pd_1/Pt_9$	0.53	1.13	1.52	1.36	1.36	3.22	3.28	2.31	2.34	3.10	3.11	2.37	2.34
$EG^{1O}/Pt_8Pd_1/Pt_9$	0.29	1.24	−0.52	1.70	1.91	3.17	3.98	2.28	3.41	2.92	3.77	2.41	3.18
$EG^{2O}/Pt_9/Pt_8Pd_1$	0.51	1.45	1.41	1.35	1.49	3.28	3.27	2.35	2.36	3.11	3.08	2.36	2.35
$EG^{1O}/Pt_9/Pt_8Pd_1$	0.44	1.70	−0.49	2.12	1.99	3.21	3.98	2.27	3.40	2.91	3.77	2.35	3.17

Table S8: Angle between the C−C axis and the surface normal, $\alpha_{CC\perp}$, and percent variations, with respect to gas-phase ethylene glycol, in the OCC and HOC angles, as well as in OCCO and HOCC dihedral angles for ethylene glycol adsorbed on undoped and doped substrates.

System/Pt(100)	$\alpha_{CC\perp}$ (°)	$\Delta_{O_1C_1C_2}$	$\Delta_{O_2C_2C_1}$	$\Delta_{H_1O_1C_1}$	$\Delta_{H_2O_2C_2}$ (%)	$\Delta_{O_1C_1C_2O_2}$	$\Delta_{H_1O_1C_1C_2}$	$\Delta_{H_2O_2C_2C_1}$
EG^{2O}	88.8	−0.2	−0.3	0.7	0.6	51.5	2.5	2.4
EG^{1O}	55.6	−3.0	−0.9	−2.9	1.8	−35.0	−49.1	−2.2
$EG^{2O}/Pt_8Fe_1/Pt_9$	88.0	0.4	0.3	0.8	0.6	43.6	0.6	−1.5
$EG^{1O}/Pt_8Fe_1/Pt_9$	54.8	−2.9	−0.9	−2.8	1.7	−36.7	−51.4	−2.0
$EG^{2O}/Pt_9/Pt_8Fe_1$	89.0	0.0	−0.3	0.5	0.8	50.0	2.2	2.2
$EG^{1O}/Pt_9/Pt_8Fe_1$	55.5	−2.8	−0.9	−2.8	1.7	−34.8	−50.0	−2.4
$EG^{2O}/Pt_8Co_1/Pt_9$	88.2	0.4	0.1	0.8	0.6	42.3	3.0	−0.9
$EG^{1O}/Pt_8Co_1/Pt_9$	52.7	−2.1	−0.7	−2.1	1.7	−34.1	−51.2	−4.5
$EG^{2O}/Pt_9/Pt_8Co_1$	89.0	0.1	−0.1	0.6	0.7	49.4	2.0	1.8
$EG^{1O}/Pt_9/Pt_8Co_1$	55.5	−2.9	−0.9	−2.8	1.8	−35.0	−50.4	−2.3
$EG^{2O}/Pt_8Ni_1/Pt_9$	85.5	0.5	0.4	0.5	0.5	40.3	6.1	−2.8
$EG^{1O}/Pt_8Ni_1/Pt_9$	51.7	−2.1	−0.6	−2.2	1.7	−35.1	−49.7	−3.8
$EG^{2O}/Pt_9/Pt_8Ni_1$	89.0	0.2	0.1	0.7	0.7	48.2	1.7	1.7
$EG^{1O}/Pt_9/Pt_8Ni_1$	55.4	−2.9	−0.9	−2.8	1.8	−35.5	−50.0	−2.4
$EG^{2O}/Pt_8Ru_1/Pt_9$	88.1	0.7	0.0	0.3	0.7	42.2	6.4	−1.8
$EG^{1O}/Pt_8Ru_1/Pt_9$	54.5	−3.2	−0.8	−3.1	2.0	−42.9	−59.7	−0.5
$EG^{2O}/Pt_9/Pt_8Ru_1$	88.7	0.1	−0.1	0.5	0.6	51.0	2.7	2.1
$EG^{1O}/Pt_9/Pt_8Ru_1$	55.3	−2.9	−0.8	−2.7	1.7	−35.9	−51.0	−3.4
$EG^{2O}/Pt_8Rh_1/Pt_9$	89.2	0.5	0.0	0.4	0.7	45.2	4.5	−0.3
$EG^{1O}/Pt_8Rh_1/Pt_9$	54.5	−3.0	−0.9	−3.0	1.9	−38.7	−53.7	−1.8
$EG^{2O}/Pt_9/Pt_8Rh_1$	88.9	−0.2	−0.3	0.8	0.7	50.2	3.0	2.9
$EG^{1O}/Pt_9/Pt_8Rh_1$	55.4	−2.8	−0.9	−2.8	1.7	−35.7	−50.2	−2.9
$EG^{2O}/Pt_8Pd_1/Pt_9$	89.4	−0.3	0.0	0.7	0.7	50.9	1.8	3.0
$EG^{1O}/Pt_8Pd_1/Pt_9$	55.8	−2.3	−0.9	−2.4	1.6	−31.0	−47.8	−4.1
$EG^{2O}/Pt_9/Pt_8Pd_1$	88.9	−0.1	−0.2	0.6	0.6	51.1	2.4	2.3
$EG^{1O}/Pt_9/Pt_8Pd_1$	55.5	−2.9	−0.9	−2.9	1.8	−35.0	−49.4	−2.3

10 Density of States for the Adsorption of Ethylene Glycol

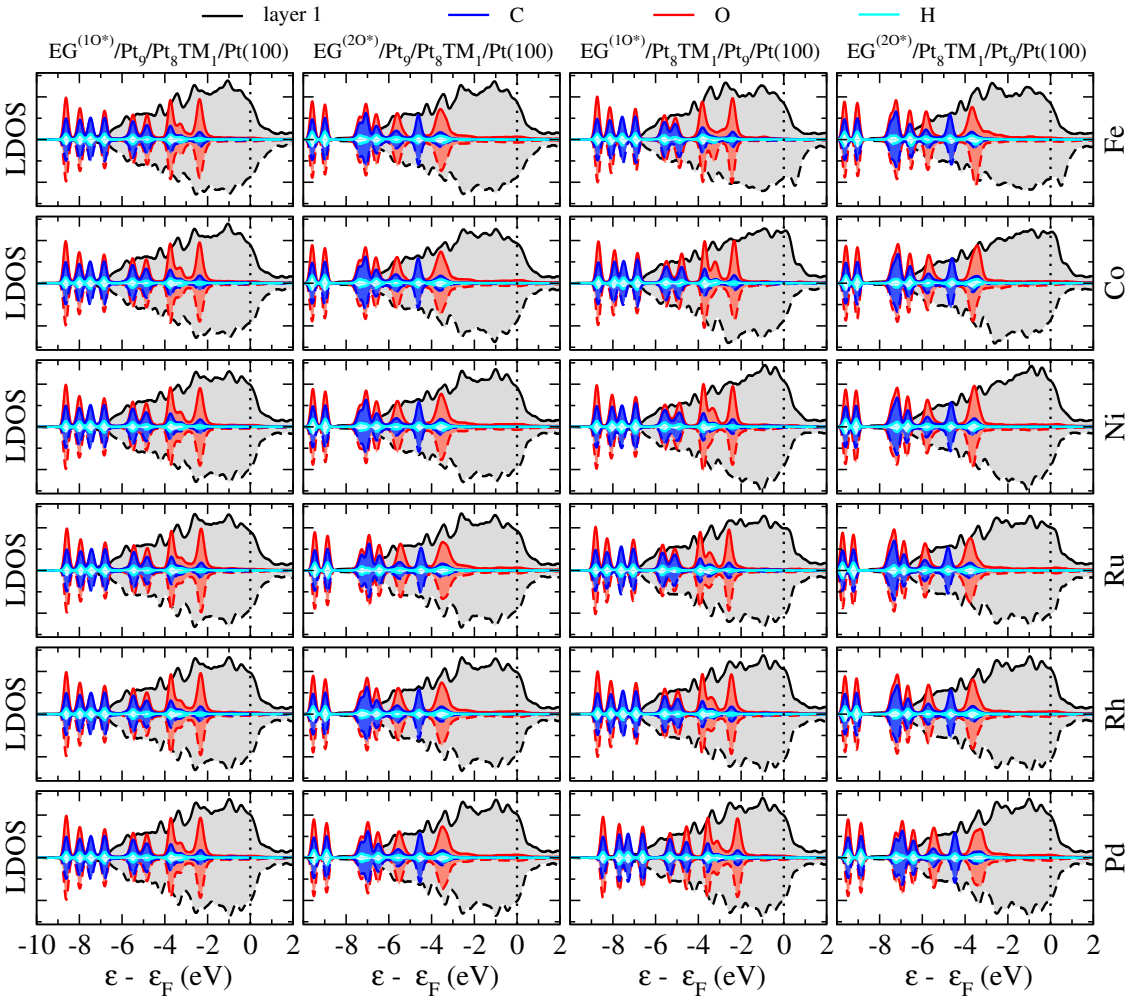

Figure S19: Average local density of states (LDOS) per atom of the EG and per atom of the two topmost layers of substrate for EG/Pt_8TM_1(100) lowest energies configurations, in which the EG adsorbs with one (1O*) or two (2O*) O atoms. The vertical dashed lines indicate the Fermi level.

11 Effective Bader Charges on Dopant Atoms upon Ethylene Glycol Adsorption

The effective Bader charge on the TM dopants in adsorbed systems are presented in Table S9.

Table S9: Effective charges in the adsorbed systems, in e: the charge on TM, Q_{eff}^{TM}; the average charge on surface Pt atoms, $Q_{eff}^{Pt(sur)}$; the average charge on subsurface Pt atoms, $Q_{eff}^{Pt(sub)}$; the sum of the charges on-surface layer, Q_{eff}^{sur}; the sum of the charges on-subsurface layer, Q_{eff}^{sub}; and the charge on ethylene glycol, Q_{eff}^{EG}.

System/Pt(100)	Q_{eff}^{TM}	$Q_{eff}^{Pt(sur)}$	$Q_{eff}^{Pt(sub)}$	Q_{eff}^{sur}	Q_{eff}^{sub}	Q_{eff}^{EG}
			e			
$EG^{2O}/Pt_8Fe_1/Pt_9$	0.91	−0.13	0.00	−0.12	0.03	0.08
$EG^{1O}/Pt_8Fe_1/Pt_9$	0.94	−0.13	0.01	−0.10	0.05	0.03
$EG^{2O}/Pt_9/Pt_8Fe_1$	0.92	−0.10	0.01	−0.86	0.99	0.16
$EG^{1O}/Pt_9/Pt_8Fe_1$	0.92	−0.09	0.01	−0.83	1.01	0.10
$EG^{2O}/Pt_8Co_1/Pt_9$	0.69	−0.11	0.01	−0.20	0.10	0.10
$EG^{1O}/Pt_8Co_1/Pt_9$	0.71	−0.11	0.01	−0.18	0.11	0.05
$EG^{2O}/Pt_9/Pt_8Co_1$	0.68	−0.09	0.02	−0.77	0.83	0.16
$EG^{1O}/Pt_9/Pt_8Co_1$	0.69	−0.08	0.02	−0.74	0.85	0.10
$EG^{2O}/Pt_8Ni_1/Pt_9$	0.49	−0.10	0.02	−0.30	0.17	0.12
$EG^{1O}/Pt_8Ni_1/Pt_9$	0.50	−0.10	0.02	−0.28	0.19	0.07
$EG^{2O}/Pt_9/Pt_8Ni_1$	0.46	−0.08	0.03	−0.69	0.68	0.16
$EG^{1O}/Pt_9/Pt_8Ni_1$	0.50	−0.07	0.03	−0.67	0.72	0.11
$EG^{2O}/Pt_8Ru_1/Pt_9$	0.50	−0.10	0.02	−0.33	0.21	0.15
$EG^{1O}/Pt_8Ru_1/Pt_9$	0.52	−0.10	0.03	−0.31	0.23	0.09
$EG^{2O}/Pt_9/Pt_8Ru_1$	0.48	−0.08	0.03	−0.69	0.69	0.15
$EG^{1O}/Pt_9/Pt_8Ru_1$	0.48	−0.07	0.03	−0.66	0.69	0.10
$EG^{2O}/Pt_8Rh_1/Pt_9$	0.31	−0.09	0.03	−0.43	0.27	0.15
$EG^{1O}/Pt_8Rh_1/Pt_9$	0.33	−0.09	0.03	−0.40	0.28	0.10
$EG^{2O}/Pt_9/Pt_8Rh_1$	0.27	−0.07	0.03	−0.62	0.53	0.16
$EG^{1O}/Pt_9/Pt_8Rh_1$	0.26	−0.07	0.03	−0.59	0.54	0.10
$EG^{2O}/Pt_8Pd_1/Pt_9$	0.21	−0.08	0.03	−0.45	0.29	0.14
$EG^{1O}/Pt_8Pd_1/Pt_9$	0.24	−0.08	0.03	−0.42	0.30	0.08
$EG^{2O}/Pt_9/Pt_8Pd_1$	0.17	−0.07	0.04	−0.59	0.47	0.16
$EG^{1O}/Pt_9/Pt_8Pd_1$	0.17	−0.06	0.04	−0.56	0.47	0.11

12 Electronegativity of the atoms

The Pauli electronegativity for all atoms involved in our study are provided in Table S10.

Table S10: Electronegativity of the atoms involved in our study.

Chemical species	H	C	O	Fe	Co	Ni	Ru	Rh	Pd	Pt
Electronegativity	2.2	2.6	3.4	1.8	1.9	1.9	2.2	2.3	2.2	2.3

13 Adsorption energy versus *d*-band center

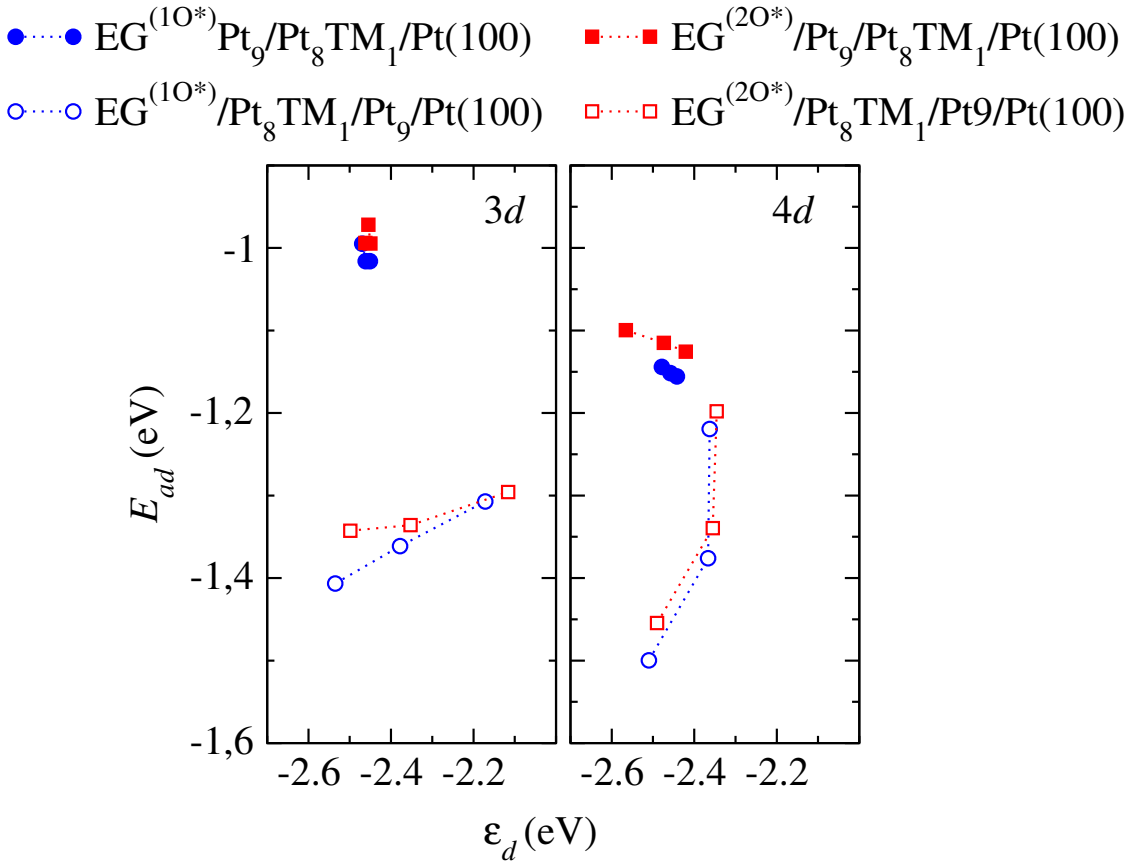

Figure S20: Relationship between the adsorption energy E_{ad} and the average *d*-band center of the occupied *d*-states for TM atoms interacting with the molecule for the lowest energy configurations that differ in the number of atoms adsorbed on surfaces and in the two types of substrates (with the dopant positions on surface and subsurface).